Abstract

Diffraction coefficients are derived for a thin dielectric half-plane and strip having arbitrary permittivity and permeability. This is accomplished by modeling the thin material layer by a pair of modified resistive and conductive sheets. Using this model, the dielectric half-plane is first treated via the dual integral equation approach. By employing the half-plane solution, up to third order multiply diffracted fields are then derived for the case of a strip. The latter are obtained via the extended spectral ray method and include the surface wave diffraction effects in a uniform manner. Numerical results are also presented which validate the accuracy of the model and that of the derived diffraction coefficients.

TABLE OF CONTENTS

I. Introduction

It was recently suggested in *Senior and Volakis [1987]* that a thin dielectric layer of given permittivity and permeability can be effectively modeled by a pair of modified resistive and conductive sheets each satisfying given boundary conditions. These define a set of electric and magnetic currents and are an improvement over the traditional resistive and conductive sheets *[Senior; 1985]*. More precisely, they have already been shown to provide an accurate modeling in the case of thin non-magnetic dielectric layers *[Senior and Volakis, 1987; Volakis and Senior, 1987]* and we expect this to also hold for the more general case. In this paper we consider the problem of diffraction by a thin dielectric half-plane and strip having arbitrary permittivity and permeability. Such canonical geometries are of interest because they occur on airborne vehicles and can also be found on antennas. Thus, they are important in the development of general scattering and radiation codes.

The first part of the paper deals with the half-plane problem. Using the dual integral equation approach *[Clemmow, 1951; Volakis and Ricoy, 1987]*, a solution for the scattered field is derived satisfying the boundary conditions defining the modified resistive and conductive sheets. The resultant integral is then evaluated asymptotically to obtain the diffraction coefficient for the dielectric half-plane and is important to note that this result is in terms of well known and easily evaluated functions.

The rest of the paper is concerned with the scattering by a strip. Particularly, we obtain all diffraction and surface wave contributions up to and including third order interactions. These contributions are derived via the application of the extended

spectral ray method (ESRM) *[Herman and Volakis, 1987; Tiberio and Kouyoumjian, 1979]*. Unlike the slope diffraction approach *[Kouyoumjian, etc., 1981]*, this method is rigorous and has thus been shown to produce very accurate results.

II. Mathematical Formulation

A plane wave is incident in the plane perpendicular to the edge of a thin dielectric half-plane occupying the xz plane as shown in Fig. 1. The incident wave is assumed H-polarized (the E-polarization case can be treated via duality) having the form

$$H_z^i = e^{jk(x\cos\phi_o + y\sin\phi_o)}$$

$$E_x^i = Z\sin\phi_o \, H_z^i$$

$$E_y^i = -Z\cos\phi_o \, H_z^i \tag{1}$$

where $Z = 1/Y$ is the intrinsic free space impedance and a time factor of $e^{j\omega t}$ has been assumed and suppressed.

As shown in *Senior and Volakis [1987]*, the material half-plane can be modeled by a pair of coincident electric and magnetic current sheets satisfying the boundary conditions

$$Y\left(\frac{1}{\eta_e} + \frac{1}{\eta_m}\right)\left(E_x^+ + E_x^-\right) - \frac{1}{jk\eta_m}\frac{\partial}{\partial y}\left(H_z^+ + H_z^-\right) = H_z^+ - H_z^- \tag{2}$$

$$Z\left(\frac{1}{\eta_m^*} + \frac{1}{\eta_e^*}\right)\left(H_z^+ + H_z^-\right) - \frac{1}{jk\eta_e^*}\frac{\partial}{\partial y}\left(E_x^+ + E_x^-\right) = E_x^+ - E_x^- \quad . \tag{3}$$

An alternate form of these also appears in *Weinstein* [1969]. In (2) - (3), the plus and minus superscripts denote the fields on the upper and lower surfaces of the sheets, respectively. Also,

$$\eta_e = \frac{-2j}{k\tau(\varepsilon-1)} \qquad \eta_m = \frac{-2j\mu}{k\tau(\mu-1)} \tag{4}$$

$$\eta_e^* = \frac{-2j\varepsilon}{k\tau(\varepsilon-1)} \qquad \eta_m^* = \frac{-2j}{k\tau(\mu-1)} \tag{5}$$

where τ denotes the thickness of the simulated half-plane, ε is the relative permittivity of the dielectric and μ is the corresponding relative permeability. It is further noted that the superscript * in (5) is only notational and does not imply the complex conjugate of the quantities in (4). In the following, the dual integral equation approach is employed for the solution of the scattered fields rather than the traditional Wiener-Hopf technique. The reason for this choice is that the dual integral equation approach or angular spectrum method as referred to by *Clemmow [1951]* requires less steps to arrive at the final solution.

The electric and magnetic currents implied by (2) and (3) are given by

$$J_x^e = \left[H_z^+ - H_z^-\right], \tag{6}$$

$$J_z^m = \left[E_x^+ - E_x^-\right], \tag{7}$$

respectively. Since these lie on a plane, their scattered fields can be represented by an angular spectrum of planes waves as discussed by *Booker and Clemmow [1950] and Clemmow [1951]*. Specifically, the fields due to the above currents may be represented as

$$H_z^s = \int_C \left[\pm P^e(\cos\alpha) + P^m(\cos\alpha)\right] e^{-jk\rho\cos(\phi\mp\alpha)}\, d\alpha; \quad y \gtrless 0$$

$$E_x^s = \frac{Z}{jk}\frac{\partial H_z}{\partial y} = Z\int_C \sin\alpha\left[-P^e(\cos\alpha) \mp P^m(\cos\alpha)\right] e^{-jk\rho\cos(\phi\mp\alpha)}\, d\alpha; \quad y \gtrless 0$$

where C is the path over which $\cos\alpha$ runs from ∞ to $-\infty$ as shown in Fig. 2 and $P^e(\cos\alpha)$ with $P^m(\cos\alpha)$ are unknown spectra proportional to the angular spectra of the electric and magnetic currents, respectively. In addition, as shown in Fig. 1, (ρ,ϕ) are the polar coordinates of the observation point.

The total fields in the presence of the dielectric half-plane are now given by

$$H_z = H_z^i + H_z^s$$

$$E_x = E_x^i + E_x^s \tag{9}$$

and when these are substituted in the boundary conditions (2)-(3) the decoupled integral equations

$$\int_C \sin\alpha \left(\eta_1 + \frac{1}{\sin\alpha}\right) P^e(\cos\alpha) e^{-jkx\cos\alpha} d\alpha = \frac{\eta_m}{\eta_e(\eta_m - 1)} \sin\phi_o \, e^{jkx\cos\phi_o} \quad ; \; x>0 \tag{10}$$

$$\int_C \sin^2\alpha \left(\frac{1}{\eta_e^*} - \frac{1}{\sin\alpha} - \frac{1}{\eta^* \sin^2\alpha}\right) P^m(\cos\alpha) e^{-jkx\cos\alpha} d\alpha = \left(\frac{1}{\eta^*} - \frac{\sin^2\phi_o}{\eta_e^*}\right) e^{jkx\cos\phi_o} \quad ; \; x>0 \tag{11}$$

are obtained, where

$$\eta_1 = \frac{\eta_m + \eta_e}{\eta_e(\eta_m - 1)}, \quad \frac{1}{\eta^*} = \frac{1}{\eta_e^*} + \frac{1}{\eta_m^*}. \tag{12}$$

The decoupling of (2) and (3) was, of course, expected as a consequence of the mutual independence between planar electric and magnetic currents *[Senior, 1985]*.

By imposing the conditions requiring continuity of the tangential E and H fields across the $x<0$ $(y=0)$ half plane, it is

further obtained that

$$\int_C P^e(\cos\alpha) e^{-jkx\cos\alpha} d\alpha = 0; \quad x<0 \tag{13}$$

$$\int_C \sin\alpha \; P^m(\cos\alpha) e^{-jkx\cos\alpha} d\alpha = 0; \quad x<0 \tag{14}$$

The unknown spectrum $P^e(\cos\alpha)$ can now be uniquely determined from the solution of the dual set of integral equations (10) and (13) whereas $P^m(\cos\alpha)$ can be determined from a solution of (11) and (14).

III. Solution of the Integral Equations

The procedure for solving the integral equations (10) and (13) or (11) and (14) follows that already discussed in *Clemmow [1951]*. The reader is also referred to *Volakis and Ricoy [1987]* or *Volakis [1987]* for a more extensive application of the method. Below we consider the solution of each independent set of equations. As will be seen, the solution of (10) and (13) is rather straightforward and the result is similar to that given by *Senior [1952]* in the treatment of the impedance half-plane via the Wiener-Hopf technique. The solution of (11) and (14) requires similar steps. However, the correct solution is obtained only after application of a physical condition relating to the relevant half plane current behavior.

A. Solution of Equations (10) and (13)

To solve (10) and (13) for $P^e(\cos\alpha)$, the integration variable is first transformed to $\lambda = \cos\alpha$. In so doing, we obtain

$$\int_{-\infty}^{\infty} \left(\eta_1 + \frac{1}{\sqrt{1-\lambda^2}} \right) P^e(\lambda) e^{-jkx\lambda} d\lambda = \frac{\eta_m}{\eta_e(\eta_m - 1)} \sqrt{1-\lambda_o^2}\ e^{jkx\lambda_o};\ x>0 \qquad (15)$$

$$\int_{-\infty}^{\infty} \frac{P^e(\lambda)}{\sqrt{1-\lambda^2}} e^{-jkx\lambda} d\lambda = 0;\ x<0 \qquad (16)$$

where $\lambda_0 = \cos\phi_0$. Since (16) is valid for $x<0$, the path of integration may be closed by a semi-infinite contour in the upper half of the λ-plane without effecting the value of the integral. By the residue theorem we then deduce that $P^e(\lambda)/\sqrt{1-\lambda^2}$ is a function free of zeros and poles (i.e. regular) in the upper half of the λ-plane. This implies that $P^e(\lambda)$ can be expressed as

$$P^e(\lambda) = \sqrt{1+\lambda}\ U^e(\lambda) \qquad (17)$$

where $U^e(\lambda)$ is an unknown function regular in the upper half of the λ-plane. Similarly, the path of integration in (15) can be closed by a semi-infinite contour in the lower half of the λ-plane and by applying the residue theorem we obtain

$$\left\{ K_+(\lambda;\eta_1) K_-(\lambda;\eta_1) \right\}^{-1} P^e(\lambda) = -\frac{1}{2\pi j} \frac{\eta_m}{\eta_e(\eta_m-1)} \frac{\sqrt{1-\lambda_o^2}}{\lambda+\lambda_0} \frac{L^e(\lambda)}{L^e(-\lambda_0)} \qquad (18)$$

where $L^e(\lambda)$ is again an unknown function regular in the lower half

of the λ-plane and $K_+(\lambda;\eta_1) = K_-(-\lambda;\eta_1)$ is the Wiener-Hopf split function satisfying *[Senior, 1952]*.

$$\left(\eta_1 + \frac{1}{\sqrt{1-\lambda^2}}\right)^{-1} = K_+(\lambda;\eta_1)K_-(\lambda;\eta_1)\,. \tag{19}$$

The K_+ function is regular in the upper half of the λ-plane and is given by

$$K_+(\cos\alpha;\eta = \frac{4}{\sqrt{\eta}}\sin\alpha/2\left\{\frac{\Psi_\pi(3\pi/2-\alpha-\theta)\ \Psi_\pi(\pi/2-\alpha+\theta)}{\Psi_\pi^2(\pi/2)}\right\}^2$$
$$\left\{\left(1+\sqrt{2}\ \cos\left(\frac{\pi/2-\alpha+\theta}{2}\right)\right)\left(1+\sqrt{2}\ \cos\left(\frac{3\pi/2-\alpha-\theta}{2}\right)\right)\right\}^{-1} \tag{20a}$$

with $\sin\theta = 1/\eta$ and Ψ_π being the *Maliuzhinets [1958]* function. In its exact form this is an integral with infinite limits. However, it can be approximated very accurately by the expressions *[Volakis and Senior, 1985]*

$$\Psi_\pi(z) \approx 1-0.0129z^2 \qquad \mathrm{Imag}(z) \le 4.2$$
$$\Psi_\pi(z) \approx 1.0139z^2\left\{\cos\frac{1}{4}(z-j\ln 2)\right\}^2\exp\left\{\frac{jz}{2\pi}e^{jz}\right\} \qquad \mathrm{Imag}(z) > 4.2 \tag{20b}$$

provided $\mathrm{Re}(z) < \pi/2$; otherwise certain identities must be invoked as noted in *Volakis and Senior [1985]*.

Substituting (17) into (18) we conclude that

$$L^e(\lambda) = \sqrt{1+\lambda}\,/K_-(\lambda;\eta_1) \tag{20}$$

since $L^e(\lambda)$ and $U^e(\lambda)$ are associated with different regions of regularity. This implies

$$P^e(\lambda) = -\frac{1}{2\pi j}\,\frac{\eta_m}{\eta_e(\eta_m-1)}\,\frac{\sqrt{1+\lambda_o}\,\sqrt{1+\lambda}}{\lambda+\lambda_o}\,K_+(\lambda;\eta_1)K_+(\lambda_o;\eta_1) \tag{21}$$

as the solution of (10) and (13).

B. Solution of Equations (11) and (14)

To solve (11) and (14) for $P^m(\cos\alpha)$ we again need to transform the integration variable to $\lambda=\cos\alpha$ giving

$$\int_{-\infty}^{\infty}\sqrt{1-\lambda^2}\left(\eta_1^*+\frac{1}{\sqrt{1-\lambda^2}}\right)\left(\eta_2^*+\frac{1}{\sqrt{1-\lambda^2}}\right)P^m(\lambda)e^{-jkx\lambda}d\lambda = -\eta^*\left(\frac{1}{\eta^*}-\frac{1-\lambda_o^2}{\eta_e^*}\right)e^{jkx\lambda_o};\ x>0$$

$$\int_{-\infty}^{\infty}P^m(\lambda)e^{-jkx\lambda}d\lambda = 0;\ x<0 \tag{23}$$

where

$$\eta_{1,2}^* = \frac{\eta^*}{2}\left\{1\pm\sqrt{1+\left(\frac{4}{\eta^*\eta_e^*}\right)}\right\} \tag{24}$$

resulting from the factorization of the term multiplying $P^m(\cos\alpha)$ in (11).

Since (23) is valid for $x<0$ we can proceed as in the previous subsection and close the path of integration by a semi-infinite contour in the upper half of the λ-plane implying that

$$P^m(\lambda) = U^m(\lambda)$$

where $U^m(\lambda)$ is an unknown function regular in the upper half of the λ-plane. Similarly, the path of integration in (22) can be closed by a semi-infinite contour in the lower half of the λ-plane. In so doing and by a subsequent application of the residue theorem one concludes that

$$\sqrt{1-\lambda^2}\left\{K_+(\lambda;\eta_1^*)K_+(\lambda;\eta_2^*)K_-(\lambda;\eta_1^*)K_-(\lambda;\eta_2^*)\right\}^{-1} U^m(\lambda) = \frac{\eta^*}{2\pi j}\left\{\frac{1}{\eta_m^*}+\frac{\lambda_0^2\left[1+(\lambda+\lambda_0)A\right]}{\eta_e^*}\right\}\frac{1}{\lambda+\lambda_0}\frac{L^m(\lambda)}{L^m(-\lambda_0)},$$

where $L^m(\lambda)$ is again an unknown function regular in the lower half of the λ-plane and A is a constant. The introduction of this constant is not necessary for satisfying the solution of (22) but its presence here is related to the physical behavior of the implied current as discussed in *Volakis and Senior [1987]*.

Since $L^m(\lambda)$ and $U^m(\lambda)$ are associated with different regions of regularity one finds that

$$L^m(\lambda) = \frac{\sqrt{1+\lambda}}{K_-(\lambda;\eta_1^*)K_-(\lambda;\eta_2^*)}$$

implying

$$P^m(\lambda) = U^m(\lambda) = \frac{\eta^*}{2\pi j}\left\{\frac{1}{\eta_m^*} + \frac{\lambda_o^2\left[1+(\lambda+\lambda_o)A\right]}{\eta_e^*}\right\} \cdot$$

$$\cdot \frac{K_+(\lambda;\eta_1^*)K_+(\lambda;\eta_2^*)K_+(\lambda_o;\eta_1^*)K_+(\lambda_o;\eta_2^*)}{(\lambda+\lambda_o)\sqrt{1-\lambda}\sqrt{1-\lambda_o}} \cdot \qquad (25)$$

It now remains to determine the constant A so that the resulting fields have the proper physical behavior. It is first noted that (25) contains the contribution of two types of magnetic currents, i.e.

$$J_z^m = J_z^{m1} + J_z^{m2} \qquad (26)$$

so that

$$P^m(\lambda) = P^{m1}(\lambda) + P^{m2}(\lambda). \qquad (27)$$

Of these, $P^{m1}(\lambda)$ is due to the presence of nonunity relative permeability μ in the material and corresponds to the first term contained in the brackets of (25). $P^{m2}(\lambda)$ is associated with the second term in the brackets of (25) and is due to the equivalent magnetic current, J_z^{m2}, representing the actual component of the electric current $J_y^e(x)$ along the y direction of the layer *[Volakis and Senior, 1987]*. From Maxwell's equations *[Mayes, 1958]* we have that

$$J_z^{m2}(x) = -\frac{iZ}{k}\frac{\partial}{\partial x} J_y^e(x) \qquad (28)$$

and thus the Fourier transform of $J_y^e(x)$ is proportional to $P^{m2}(\lambda)/\lambda$. The presence of the pole at $\lambda=0$ will produce a contribution to $J_y^e(x)$ which is independent of x. To cancel this non-physical contribution, it is necessary to eliminate the pole at $\lambda=0$ demanding that $A = -1/\lambda_o$.

Consequently, the complete expression for $P^m(\lambda)$ is

$$P^m(\lambda) = \frac{\eta^*}{2\pi j}\left\{\frac{1}{\eta_m^*} - \frac{\lambda\lambda_o}{\eta_e^*}\right\} \frac{K_+(\lambda;\eta_1^*)K_+(\lambda;\eta_2^*)K_+(\lambda_o;\eta_1^*)K_+(\lambda_o;\eta_2^*)}{(\lambda+\lambda_o)\sqrt{1-\lambda}\sqrt{1-\lambda_o}} \quad . \tag{29}$$

IV. Singly Diffracted Field

The scattered field by the dielectric half-plane can now be found by substituting (21) and (29) into (8). After some simple manipulation this gives

$$H_z^s = \frac{j}{4\pi}\int_C \left(\sec\frac{\alpha+\phi_o}{2}+\sec\frac{\alpha-\phi_o}{2}\right)\left[\pm H_z^e(\alpha,\phi_o) + H_z^{m1}(\alpha,\phi_o) + H_z^{m2}(\alpha,\phi_o)\right] e^{-jk\rho\cos(\alpha\mp\phi)}\, d\alpha; \quad y \gtrless 0 \tag{30}$$

where

$$H_z^e(\alpha,\phi_o) = -\frac{\eta_m}{\eta_e(\eta_m-1)} K_+(\cos\alpha;\eta_1)K_+(\cos\phi_o;\eta_1) \tag{31}$$

$$H_z^{m1}(\alpha,\phi_o) = \frac{\eta^*}{\eta_m^*}\frac{K_+(\cos\alpha;\eta_1^*)K_+(\cos\phi_o;\eta_1^*)K_+(\cos\alpha;\eta_2^*)K_+(\cos\phi_o;\eta_2^*)}{\sin\alpha\sin\phi_o} \tag{32}$$

and

$$H_z^{m2}(\alpha.\phi_0) = -\frac{\eta^*}{\eta_e^*}\cot\alpha\,\cot\phi_0 K_+(\cos\alpha;\eta_1^*)K_+(\cos\phi_0;\eta_1^*)K_+(\cos\alpha;\eta_2^*)K_+(\cos\phi_0;\eta_2^*). \tag{33}$$

To find the field scattered by the material half-plane we now deform the path of integration in (30) to the steepest descent path through the saddle point $\alpha=\phi$ or $\alpha=2\pi-\phi$ depending on whether $y>0$ or $y<0$, respectively. In the deformation process we may capture the

geometrical optics poles at $\pi-\phi_o$ or $\pi+\phi_o$ and the surface wave poles at $-\theta_1$, $-\theta_1^*$ or $-\theta_2^*$, where

$$\sin\theta_1 = \frac{1}{\eta_1}\ , \quad \sin\theta_1^* = \frac{1}{\eta_1^*}\ , \quad \sin\theta_2^* = \frac{1}{\eta_2^*} \quad . \tag{34}$$

The last are associated with the split functions $K_+(\cos\alpha;\eta)$ given in (20) and may be captured only when $\phi\to 0$ or 2π. They are thus quite important in the evaluation of the scattering by the strip (especially in low loss cases) since they correspond to guided waves within the dielectric slab. However, it should be noted that for H_z-incidence only the pole at $\alpha = -\theta_1^*$ is of importance whereas in the case of E_z-incidence the critical pole is at $\alpha=-\theta_1$. The third surface wave pole at $\alpha = -\theta_2^*$ is always far from the saddle point and could be associated with a possible higher order mode in the layer. Therefore, it could be neglected in all subsequent analysis if so desired. Nevertheless, we will consider its presence just for the purpose of generality.

The residue contribution of the above mentioned poles correspond to the geometrical optics and surface wave fields. However, since they can be easily evaluated and are not of primary interest like the diffracted field, their explicit expressions are not given here. The diffracted field is now the contribution of the integral (30) over the steepest descent path. By performing a uniform evaluation *[Kouyoumjian and Pathak, 1974]* of this integral (with respect to the geometrical optics poles only) one finds that

the diffracted field for large $k\rho$ is

$$H_{z1}^{d}(\phi,\phi_o) \sim D(\phi,\phi_o)\,\frac{e^{-jk\rho}}{\sqrt{\rho}}, \tag{35}$$

where

$$D(\phi,\phi_o) = \frac{e^{-j\pi/4}}{2\sqrt{2\pi k}}\left[\sec\frac{\phi+\phi_0}{2}\,F_{kp}(2k\rho\cos^2\frac{\phi+\phi_0}{2}) + \sec\frac{\phi-\phi_0}{2}\,F_{kp}(2k\rho\cos^2\frac{\phi-\phi_0}{2})\right]$$
$$\cdot\left[H_z^{e}(\phi,\phi_o) + H_z^{m1}(\phi,\phi_o) + H_z^{m2}(\phi,\phi_o)\right] \tag{36}$$

is the diffraction coefficient and

$$F_{kp}(z) = 2j\sqrt{z}\;e^{jz}\int_{\sqrt{z}}^{\infty} e^{-j\tau^2}\,d\tau \tag{37}$$

is the transition function. A uniform evaluation of H_z^{d} with respect to the surface poles can also be performed if necessary and a procedure for accomplishing this is discussed in *Herman and Volakis [1987]*.

Letting $\rho\to\infty$ in (36) and noting that $F_{kp}(\infty) = 1$, one obtains the non-uniform diffraction coefficient

$$D^{NU}(\phi,\phi_0) = D(\phi,\phi_0)\Big|_{\rho\to\infty}$$
$$= \frac{e^{-j\pi/4}}{2\sqrt{2\pi k}}\left[\sec\frac{\phi+\phi_0}{2} + \sec\frac{\phi-\phi_0}{2}\right]\left[H_z^{e}(\phi,\phi_0)+H_z^{m1}(\phi,\phi_0)+H_z^{m2}(\phi,\phi_0)\right]. \tag{38}$$

Some typical curves of the far zone ($\rho\to\infty$) diffracted field in the presence of the half plane are given in Figure 3 for various ε and μ values.

V. Doubly Diffracted Field

Referring to the strip geometry in Figure 4, the doubly diffracted field is that which emanates from edge $Q_2(Q_1)$ after diffraction from $Q_1(Q_2)$. As illustrated in Figure 5 there are four mechanisms associated with this phenomenon and in evaluating their contribution one must consider the existence of the surface waves in addition to the diffraction ray field components. The method to be employed here will closely follow that already employed in the scattering analysis of the resistive strip *[Herman and Volakis, 1987]*. This is based on the principles of the ESRM and allows the derivation of exact integral expressions for the multiple diffracted field. These are asymptotically evaluated to obtain the higher order diffracted fields which account for surface wave field contributions and remain valid when one edge is in the transition region of the other.

Let us consider the double diffraction mechanism shown in Fig. 5(a) whose contribution is equal to that in Fig. 5(c). In this case the field is incident onto Q_1 at an angle ϕ_0, scatters toward Q_2 and then diffracts from Q_2 to the observer at an angle ϕ_2. The exact integral expression of the field scattered from Q_1 to Q_2 is given in (30) with ϕ=0 and ρ=w. As discussed in *Herman and Volakis [1987]* this integral can now be interpreted as an infinite sum of inhomogeneous plane waves emanating from Q_1. Referring to Fig. 6, if these form an angle $+\alpha$ with the top face of the strip at Q_1, they will then be incident at Q_2 forming an angle $+\alpha$ with the

bottom face of the strip or alternatively an angle $-\alpha$ with the top face at Q_2. The far zone contribution of each of these inhomogeneous plane waves is the singly diffracted field given in (35) and (38). Thus, an exact integral expression for the far zone diffracted field due to the mechanisms in Fig. 5(a) and (c) is

$$H^d_{z21}(\phi_2, \phi_0) = \frac{j}{4\pi} e^{-jkw\cos\phi_2} \frac{e^{-jk\rho}}{\sqrt{\rho}} \int_C \left(\sec\frac{\alpha+\phi_0}{2} + \sec\frac{\alpha-\phi_o}{2} \right) \cdot$$

$$\cdot \left[H^e_z(\alpha,\phi_0) + H^{m1}_z(\alpha,\phi_0) + H^{m2}_z(\alpha,\phi_0) \right] D^{NU}(-\alpha,\phi_2) e^{-jkw\cos\alpha} d\alpha \qquad (39)$$

where we have employed the reciprocity condition $D^{NU}(-\alpha,\phi_2) = D^{NU}(\phi_2-\alpha)$. The phase reference of H^d_{z21} is at Q_1 and accounts for the the exponential factor $e^{-jkw\cos\phi_2}$.

The integral in (39) can now be evaluated asymptotically via the modified Pauli-Clemmow steepest descent method. It should be noted, however, that the first term of the asymptotic expansion gives a vanishing contribution because the $K_+(\cos\alpha;\eta)$ functions have a zero at $\alpha=0$. Thus, to obtain a non-zero result one must retain the second term of the expansion. The details of the evaluation parallel those in Appendix A of *Herman and Volakis [1987]* after deforming the integration path to the steepest descent path through $\alpha=0$. For our case the relevant poles are at $\pi\pm\phi_0$, $\pi\pm\phi_2$, $-\theta_1^*$ and $-\theta_2^*$. Further, noting that the contribution of the electric and magnetic currents is uncoupled, we obtain that

$$H_{z21}^{d}(\phi_2,\ \phi_0) = H_{z21}^{de}(\phi_2,\ \phi_0) + H_{z21}^{dm}(\phi_2,\ \phi_0) \tag{40}$$

with

$$H_{z21}^{de}(\phi_2,\ \phi_0) \sim j\eta_1^2 \cos\frac{\phi_2}{2}\cos\frac{\phi_0}{2}\, K_{+c}^2(1;\eta_1) K_+(\cos\phi_2;\eta_1) K_+(\cos\phi_0;\eta_1) \frac{e^{-jkw}}{\pi k\sqrt{w}} \frac{e^{-jk\rho}}{\sqrt{\rho}}$$

$$e^{-jkw\cos\phi_2} \sum_{i=1}^{3} A_i \left[1-F_{kp}(kwa_i)\right] \tag{41}$$

and

$$H_{z21}^{dm} \sim j\eta^{*2}\left(\frac{1}{\eta_m^*} - \frac{\cos\phi_0}{\eta_e^*}\right)\left(\frac{1}{\eta_m^*} - \frac{\cos\phi_2}{\eta_e^*}\right) \frac{e^{-jkw}}{\sqrt{w}} \frac{e^{-jk\rho}}{\sqrt{\rho}}$$

$$e^{-jkw\cos\phi_2} \frac{K_+(\cos\phi_2;\eta_1^*)\ K_+(\cos\phi_0;\eta_1^*)\ K_+(\cos\phi_2;\eta_2^*) K_+(\cos\phi_0;\eta_2^*)}{16\pi k \sin\frac{\phi_0}{2}\sin\frac{\phi_2}{2}} \cdot$$

$$\cdot K_{+c}^2(1;\eta_1^*)\ K_{+c}^2(1;\eta_2^*)\ b_3 \sum_{i=1}^{4} B_i \left[1-F_{kp}(kwb_i)\right] \tag{42}$$

The constants a_i, A_i, b_i and B_i are

$$a_1 = 2\cos^2\frac{\phi_0}{2},\quad a_2 = 2\cos^2\frac{\phi_2}{2}.\quad a_3 = 2\sin^2\frac{\theta_1}{2} \tag{43}$$

$$A_1 = \frac{-1}{(a_2-a_1)(a_3-a_1)} \tag{44a}$$

$$A_2 = \frac{-1}{(a_1-a_2)(a_3-a_2)} \tag{44b}$$

$$A_3 = \frac{-1}{(a_1-a_3)(a_2-a_3)} \tag{44c}$$

$$b_1 = a_1,\quad b_2 = a_2,\quad b_3 = 2\sin^2\frac{\theta_1^*}{2},\quad b_4 = 2\sin^2\frac{\theta_2^*}{2} \tag{45}$$

$$B_1 = \frac{-b_4}{(b_2-b_1)(b_3-b_1)(b_4-b_1)} \tag{46a}$$

$$B_2 = \frac{-b_4}{(b_1-b_2)(b_3-b_2)(b_4-b_2)}, \tag{46b}$$

$$B_3 = \frac{-b_4}{(b_1-b_3)(b_2-b_3)(b_4-b_3)} \tag{46c}$$

and

$$B_4 = \frac{-b_4}{(b_1-b_4)(b_2-b_4)(b_3-b_4)} \tag{46d}$$

Also,

$$K_+(\cos\alpha;\eta) = \sin\frac{\alpha}{2}\, K_{+c}(\cos\alpha;\eta)\,. \tag{47}$$

The definition of the transition function appearing in (41) and (42) must further be generalized to complex arguments so that

$$F_{kp}(z^2) = \pm 2jze^{jz^2}\int_{\pm z}^{\infty} e^{-j\tau^2}d\tau = \pm 2jzF_c(\pm z) \tag{48}$$

with the minus sign chosen when $\frac{\pi}{4} < \arg(z) < \frac{5\pi}{4}$, otherwise the plus sign is used. Note, that $F_c(z)$ satisfies the identity

$$F_c(-z) = \sqrt{\pi}\; e^{-j\pi/4}\; e^{jz^2} - F_c(z) \tag{49}$$

which is essential in accounting for the surface wave field contributions as they propagate through the dielectric layer.

In passing we note that the contribution of the double diffraction mechanisms shown in Fig. 5(b) and (d) is simply given by $H^d_{z21}(\pi-\phi_2\,,\ \pi-\phi_0)$.

VI. Triply Diffracted Field

As shown in Fig. 7, there are eight triple diffraction mechanisms to be considered. Four emanate from edge Q_1 and each gives an equal contribution to the diffracted field. The other four emanate from edge Q_2 and likewise are of equal strength. In accordance with the ESRM, an integral representation for the triply diffracted field from Q_1 is

$$H^d_{z\,121}(\phi,\phi_0) = \frac{j}{4\pi}\int_C \left(\sec\frac{\alpha+\phi}{2} + \sec\frac{\alpha-\phi}{2}\right) H^d_{z\,21}(-\alpha,\phi_0) \cdot$$

$$\cdot\left[H^e_z(\alpha,\phi) + H^{m1}_z(\alpha,\phi) + H^{m2}_z(\alpha,\phi)\right] e^{-jkw\cos\alpha}\,d\alpha \qquad (50)$$

after invoking reciprocity. Clearly, (50) was obtained by interpreting the field incident onto Q_1 to be an inhomogeneous sum of plane waves each of which subsequently undergoes a double diffraction before returning to the observer.

To perform an asymptotic evaluation of (50) we proceed in a similar manner to that discussed for the double diffraction integral (see also Appendices A and B in *Herman and Volakis [1987]*). The relevant poles in this case are $\pi \pm \phi, -\theta_1, -\theta_1^*$ and $-\theta_2^*$. As in the double diffraction case, the first term of the asymptotic expansion of (50) is zero and we must therefore retain the second term of this expansion. Noting that the electric and magnetic current contributions are uncoupled we find that

$$H^d_{z121}(\phi,\phi_0) = H^e_{z121}(\phi,\phi_0) + H^m_{z121}(\phi,\phi_0) \qquad (51)$$

with

$$H^e_{z121}(\phi,\phi_0) \sim \eta_1^3 \cos\frac{\phi}{2}\cos\frac{\phi}{2} K^4_{+c}(1;\eta_1)\, K_+(\cos\phi;\eta_1)\, K_+(\cos\phi_0;\eta_1)\, \frac{e^{-jk\rho}}{\sqrt{\rho}}$$

$$\frac{e^{j\pi/4}\, e^{-2jkw}}{\sqrt{2}\,(k\pi)^{3/2} w}\, a_3^2\, \frac{F_{kp}(kwa_3)-F_{kp}(kwa_4)}{a_3-a_4} \sum_{i=1}^{3} A_i\left[1-F_{kp}(kwa_i)\right] \qquad (52)$$

and

$$H_{z\,121}^{m}(\phi,\phi_o) \sim -\eta_*^3 \left(\frac{1}{\eta_m^*}-\frac{1}{\eta_e^*}\right)\left(\frac{1}{\eta_m^*}-\frac{\cos\phi}{\eta_e^*}\right)\left(\frac{1}{\eta_m^*}-\frac{\cos\phi_o}{\eta_e^*}\right)\frac{e^{-jk\rho}}{\sqrt{\rho}}$$

$$\cdot k_{+c}^4(1;\eta_1^*)K_{+c}^4(1;\eta_2^*)K_+(\cos\phi;\eta_1^*)K_+(\cos\phi_o;\eta_1^*)K_{+c}(\cos\phi;\eta_2^*)K_{+c}(\cos\phi_o;\eta_2^*)$$

$$\cdot\frac{\sqrt{2}\, e^{j\pi/4} e^{-2jkw}}{128\,(k\pi)^{3/2} w}\, b_3^2 \left(\sum_{i=1}^{4} B_i\left[1-F_{kp}(kwb_i)\right]\right)\left(\sum_{j=3}^{5} C_j\left[1-F_{kp}(kwb_j)\right]\right) \qquad (53)$$

In the above,

$$a_2 = 2, \quad a_4 = 2\cos^2\frac{\phi}{2}, \qquad (54)$$

$$b_2 = 2, \quad b_5 = 2\cos^2\frac{\phi}{2}, \qquad (55)$$

$$C_3 = \frac{-b_4}{(b_4-b_3)(b_5-b_3)}, \qquad (56a)$$

$$C_4 = \frac{-b_4}{(b_3-b_4)(b_5-b_4)}, \qquad (56b)$$

$$C_5 = \frac{-b_4}{(b_5-b_3)(b_5-b_4)}, \qquad (56c)$$

and all other constants are defined in (43)-(49) with a_2 and b_2 as given in (54)-(55).

Expressions (51)-(53) give the contribution of the triply diffracted field emanating from Q_1. The triply diffracted field emanating from Q_2 is simply given by $H_{z\,121}^{d}(\pi-\phi, \pi-\phi_0)\, e^{jkw(\cos\phi+\cos\phi_0)}$ with the phase reference at Q_1.

VII. Numerical results

The sum of the fields due to the first, second and third order diffraction was found to yield a good approximation of the total (bistatic) diffracted field by the thin dielectric strip. A few backscatter and bistatic patterns are presented next. These are compared with moment method (and in one case with measured) data for the purpose of verifying their validity.

Fig. 8 presents the backscatter pattern by a strip 1.7 wavelengths wide and 1/100 of a wavelength thick. The material is that of an absorber and as seen our high frequency solution is in good agreement with the measured and numerical data *[Ricoy and Volakis, 1987]*. The agreement is maintained even near grazing (ϕ=0) where the surface wave and the multiple diffraction effects associated with the modified conductive sheet are important. Backscatter curves for other values of ε, μ and τ are given in Fig. 9. We note that for the strip corresponding to ε = 4 and μ = 1, the calculated echo width would vanish near ϕ=0 without the addition of the modified conductive sheet. The importance and relative strength of the multiply diffracted fields associated with one of the backscatter patterns in Figure 9 is illustrated in Figure 10. As seen, the backscatter contribution of the triply diffracted field is of most importance near grazing incidences. Some bistatic patterns are included in Figure 11 and they are again in good agreement with the numerical data. The individual contributions of the multiply diffracted fields corresponding to one of the bistatic patterns in Figure 11 are given in Figure 12. As expected, the doubly diffracted field is of primary importance,

particularly in the forward scatter region. In fact, for the case of grazing incidence, presented in Figure 12, the singly and doubly diffracted fields each produce cancelling infinities so that the total field remains bounded.

The third order solution given here remains valid for small strip widths down to 0.5 wavelengths or better. A more restrictive statement, however, would require a knowledge of the specific strip thickness and material parameters. The extent of the validity of the model as a function of thickness and refractive index is certainly of interest and should also be examined in the future.

VIII. Summary

In this paper a uniform diffraction coefficient was derived for a thin dielectric half-plane using an improved current sheet model. Specifically, the thin material layer characterized with arbitrary permittivity and pemeability was modeled by a pair of modified resistive and conductive sheets. The resulting integral equations were then solved via the dual integral equation approach. Using the half-plane results, diffraction coefficients were also derived via the extended spectral ray method accounting for the presence of the surface wave fields. Backscatter and bistatic patterns were also presented and found to be in good agreement with corresponding moment method data.

IX. REFERENCES

Booker, H. G. and P. C. Clemmow, "The concept of an angular spectrum of plane waves, and its relation to that of polar diagrams and aperture distribution," *Proc. Inst. Elec. Eng.*, 97, 11-17, Jan. 1950.

Clemmow, P. C., "A method for the exact solution of a class of two-dimensional diffraction problems," *Proc. Roy. Soc. A*, 205, 286-308, 1951.

Herman, M. I. and J. L. Volakis, "High frequency scattering by a resistive strip and extensions to conductive and impedance strips," *Radio. Sci.*, 22, 335-349, May-June 1987.

Kouyoumjian, R. G. and P. H. Pathak, "A uniform geometrical theory of diffraction for an edge in a perfectly conducting surface," *Proc. IEEE*, 62, 1448-1461, 1974.

Kouyoumjian, R. G., P. H. Pathak, and W. D. Burnside, "A uniform GTD for the diffraction by edges, vetics and convex surfaces," in *Theoretical Methods for Determining the Interaction of Electromagnetic Waves with Structures*, edited by J. K. Skwirzyinski, Sijthoff and Noordhoof, Alphen aan den Rijn, The Netherlands, 1981.

Maliuzhinets, G. D., "Excitation, reflection and emission of surface waves from a wedge with given face impedances," *Sov. Phys. Dokl.*, Engl. Transl., 3, 752-755, 1958.

Mayes, P.E., "The equivalence of electric and magnetic sources," *IEEE Trans. Antennas Propagat.*, AP-6, 295-296, 1958.

Ricoy, M. A. and J. L. Volakis, "Integral Equations with Reduced Unknowns for the Simulation of Two-Dimensional Composite Structures," submitted to *IEEE Trans. on Antennas and Propagat.*

Senior, T. B. A., "Diffraction by a semi-infinite metallic sheet," *Proc. Roy. Soc.* (London), 213(A), 436-458, 1952.

Senior, T. B. A., "Combined resistive and conductive sheets," *IEEE Trans. Antennas and Propagat.*, AP-33, 577-579, 1985.

Senior, T. B. A. and J. L. Volakis, "Sheet simulation of a thin dielectric layer," *Radio Sci.*, 22, Nov.-Dec. 1987 (in press)

Tiberio, R., and R. G. Kouyoumjian, "A uniform GTD solution for the diffraction by strips at grazing incidence," *Radio Sci.*, 14(6), 933-941, 1979.

Tiberio, R., G. Manara, G. Pelosi, and R. G. Kouyoumjian, "High frequency diffraction by a double wedge," *1985 IEEE AP-S Symp. Dig.*, 443-446, 1985.

Volakis, J. L. and T. B. A. Senior, "Simple expressions for a function occurring in diffraction theory," *IEEE Trans. Antennas Propagat.*, AP-33, 678-680, 1985.

Volakis, J. L. and M. A. Ricoy, "Diffraction by a thick perfectly conducting half-plane," *IEEE Trans. Antennas and Propagat.*, AP-35, 62-72, Jan. 1987.

Volakis, J. L., "Scattering by a thick impedance half plane," *Radio Sci.*, 22, 13-25, Jan.-Feb. 1987.

Volakis, J. L. and T. B. A. Senior, "Diffraction by a thin dielectric half plane," *IEEE Trans. Antennas and Propagat.*, AP-35, Dec. 1987 (in press).

Weinstein, A.L., *The Theory of Diffraction and the Factorization Method*, Golem Press, Boulder, CO., 1969.

X. APPENDIX

Diffraction by a Resistive Half-Plane and Strip Imbedded in a Dielectric Layer

The analysis of this geometry, shown in figure 13, is identical to that given for the dielectric layer provided one of the parameters is modified to account for the presence of the resistive sheet. In particular, for H_z-incidence the parameter η_e given in (4) must be replaced by η_e' , where

$$\eta_e' = \frac{\eta_e R}{\eta_e Z + 2R} = \frac{R}{Z + jRk\tau(\varepsilon-1)}$$

with R denoting the resistivity in Ohms per square of the imbedded resistive half-plane or strip. For E_z-incidence, the solution remains the same as that found for the H_z-incidence case provided we let $\varepsilon \to \mu$ and $\mu \to \varepsilon$ in accordance with duality. This implies $\eta_e \to \eta_m^*$, $\eta_m \to \eta_e^*$, $\eta_e^* \to \eta_m$, $\eta_m^* \to \eta_e$. However, the definition of η_e' remains the same since η_e' will again replace the $\eta_m^* \to \eta_e$ parameter.

XI. LIST OF FIGURES

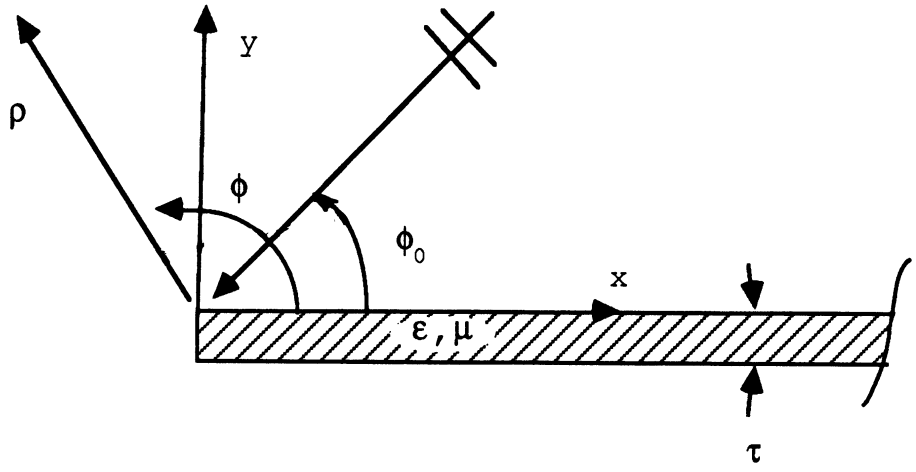

Fig. 1 Geometry of the thin dielectric half plane.

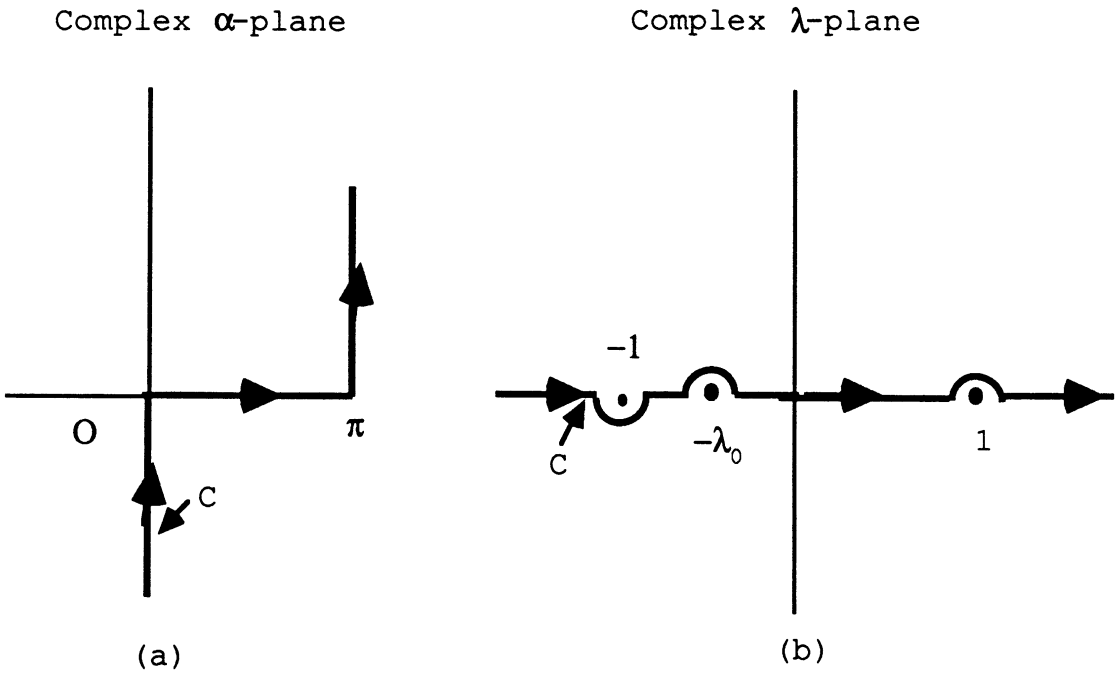

Fig. 2. Illustration of the C contour in α and λ planes

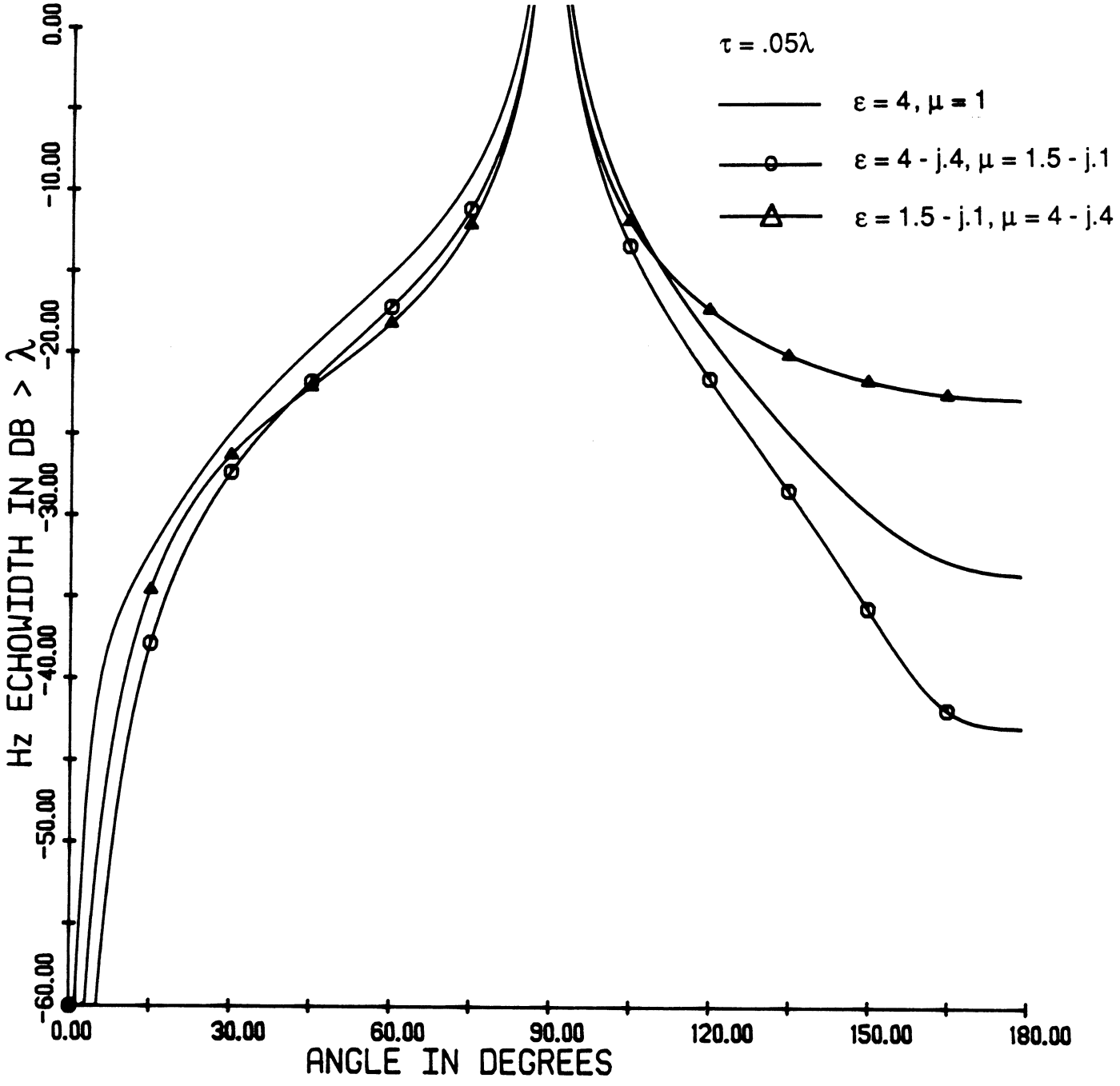

Fig. 3. H_z backscatter echowidth by three 0.05 wavelengths thick dielectric half planes characterized with the indicated values of ε and μ.

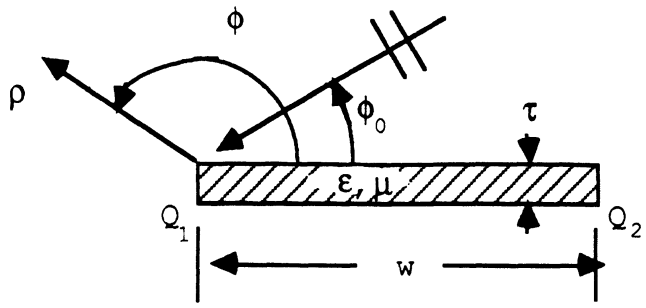

Fig. 4. Geometry of the dielectric strip.

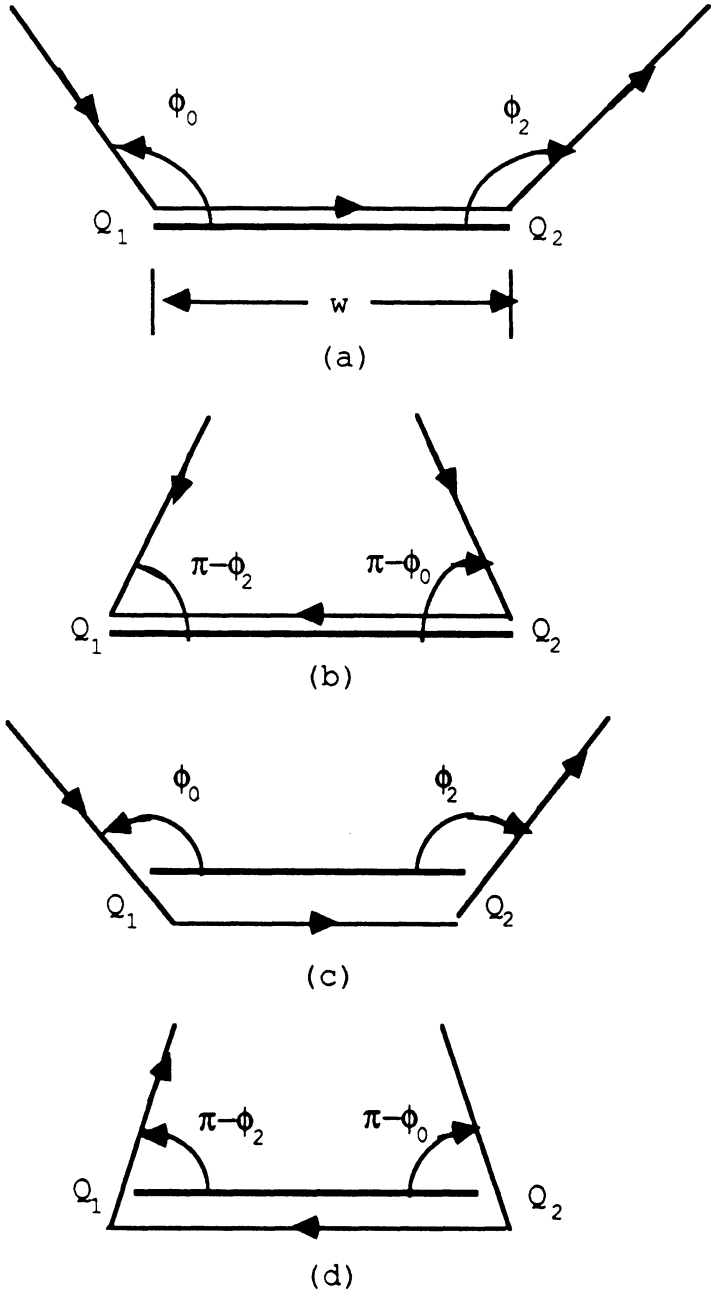

Fig. 5. Illustration of double diffraction ray mechanisms of a strip.

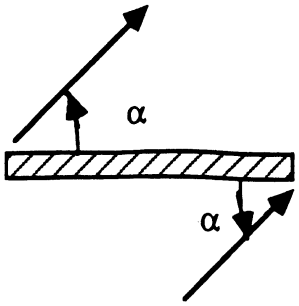

Fig. 6. Interpretation of the spectral rays.

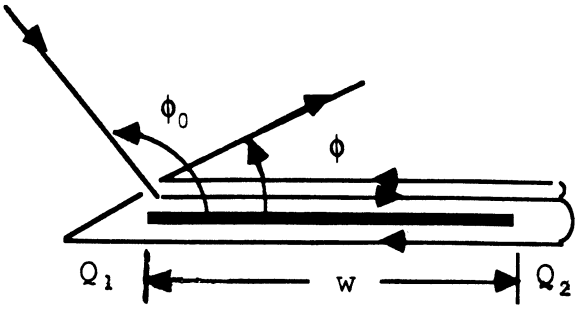

(a)

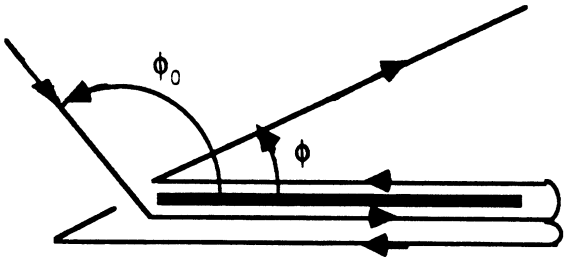

(b)

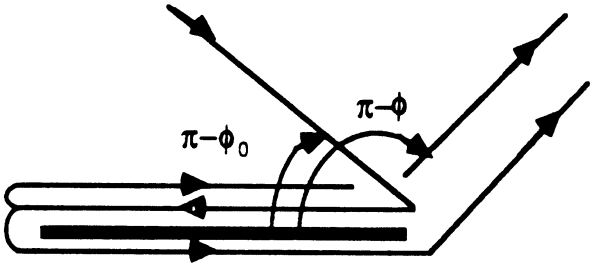

(c)

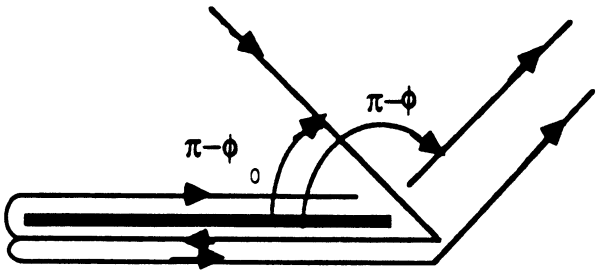

(d)

Fig. 7. Illustration of triply diffracted ray mechanisms of a strip

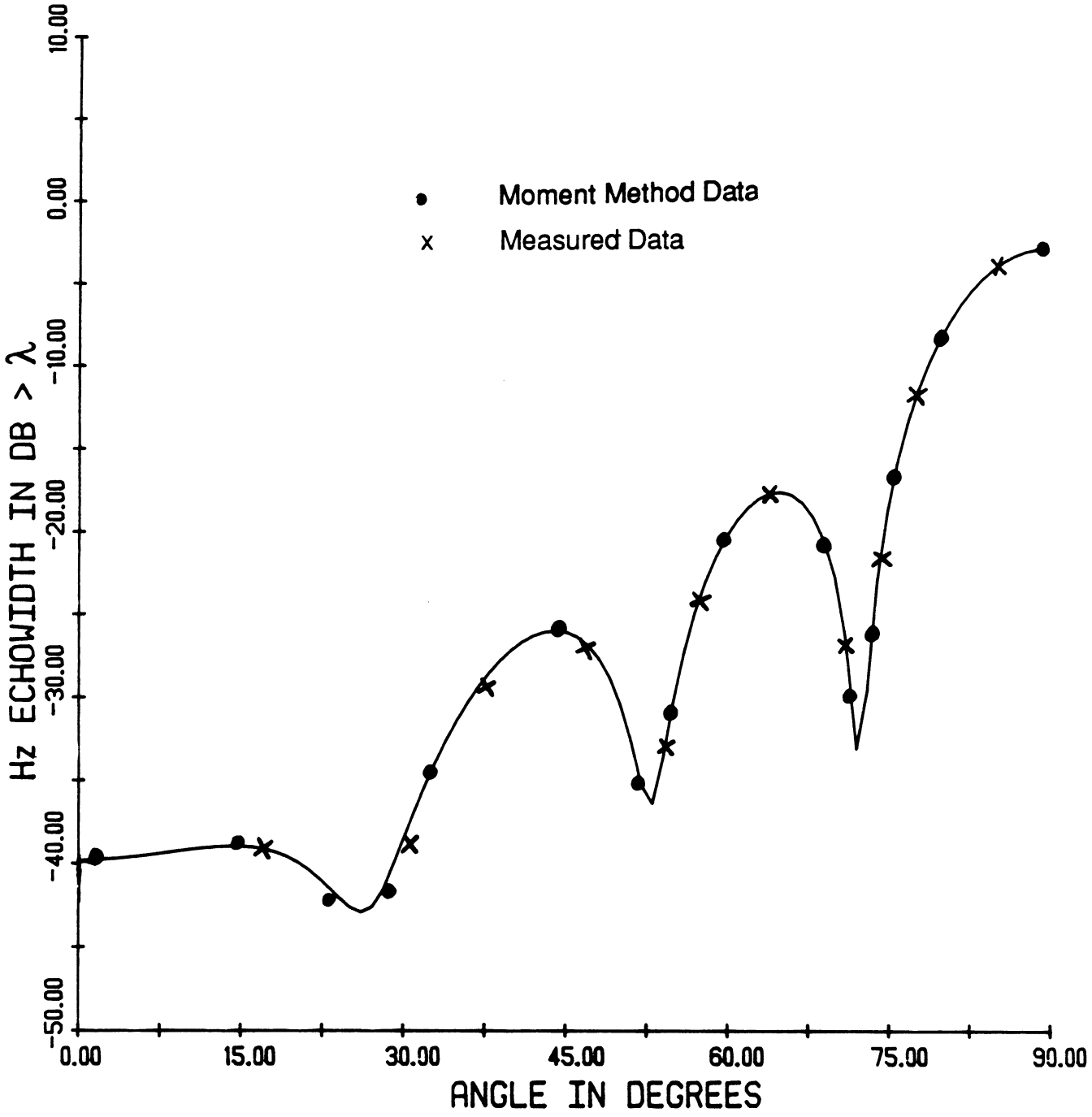

Fig. 8. H_z backscatter echowidth by a 1.7 wavelengths wide and 0.01 wavelengths thick dielectric strip having $\varepsilon = 7.4 - j1.11$ and $\mu = 1.4 - j.672$; comparison of high frequency, moment method and measured results.

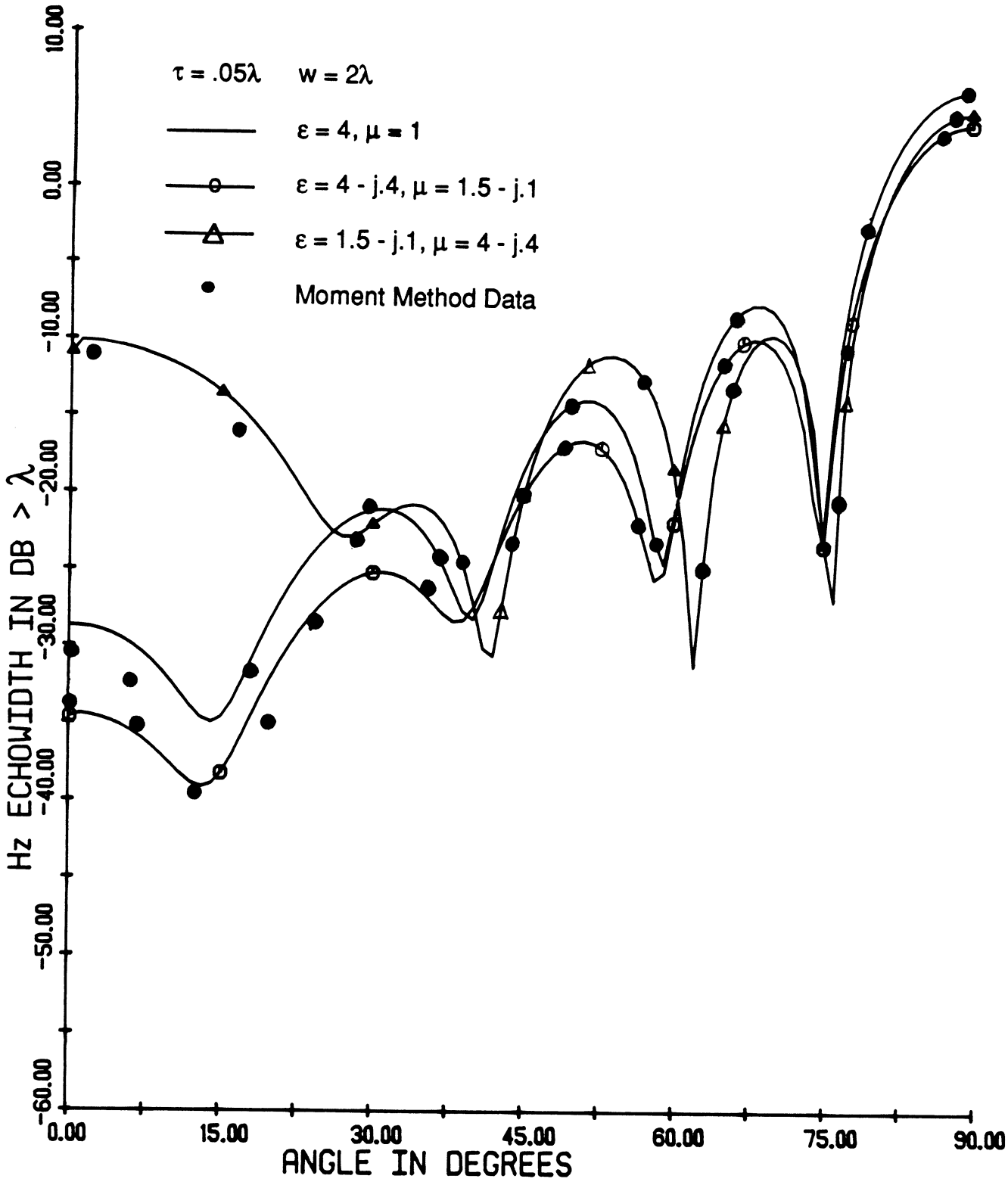

Fig. 9. H_z backscatter echowidth comparison of the high frequency solution versus moment method data for 2 wavelengths wide and .05 wavelengths thick dielectric strips with ε and μ as indicated.

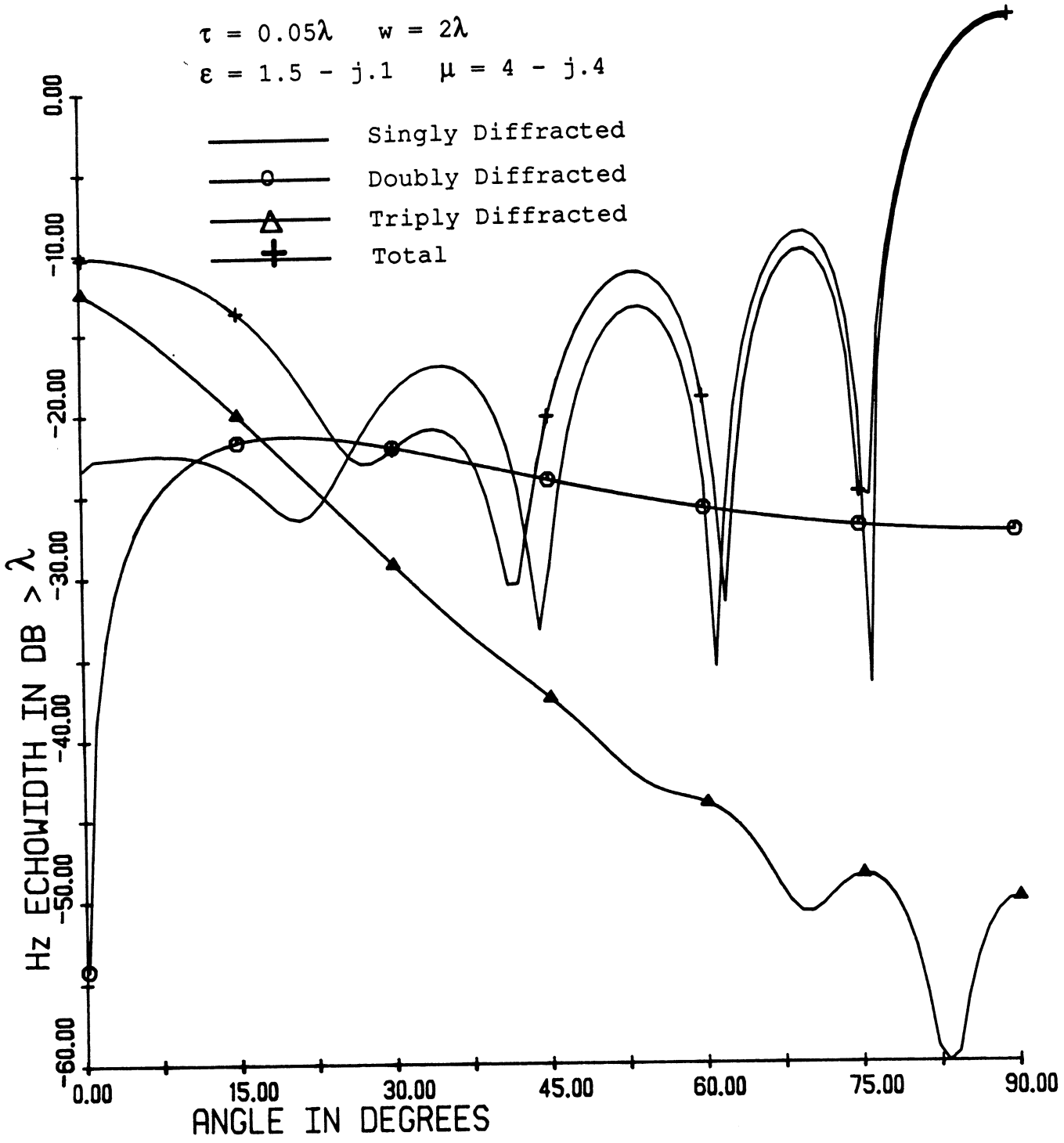

Fig. 10. Backscatter contribution of the multiply diffracted fields for the case of H_z-incidence on a 2 wavelengths wide and .05 wavelengths thick dielectric strip having $\varepsilon = 1.5 - j0.1$ and $\mu = 4 - j.4$.

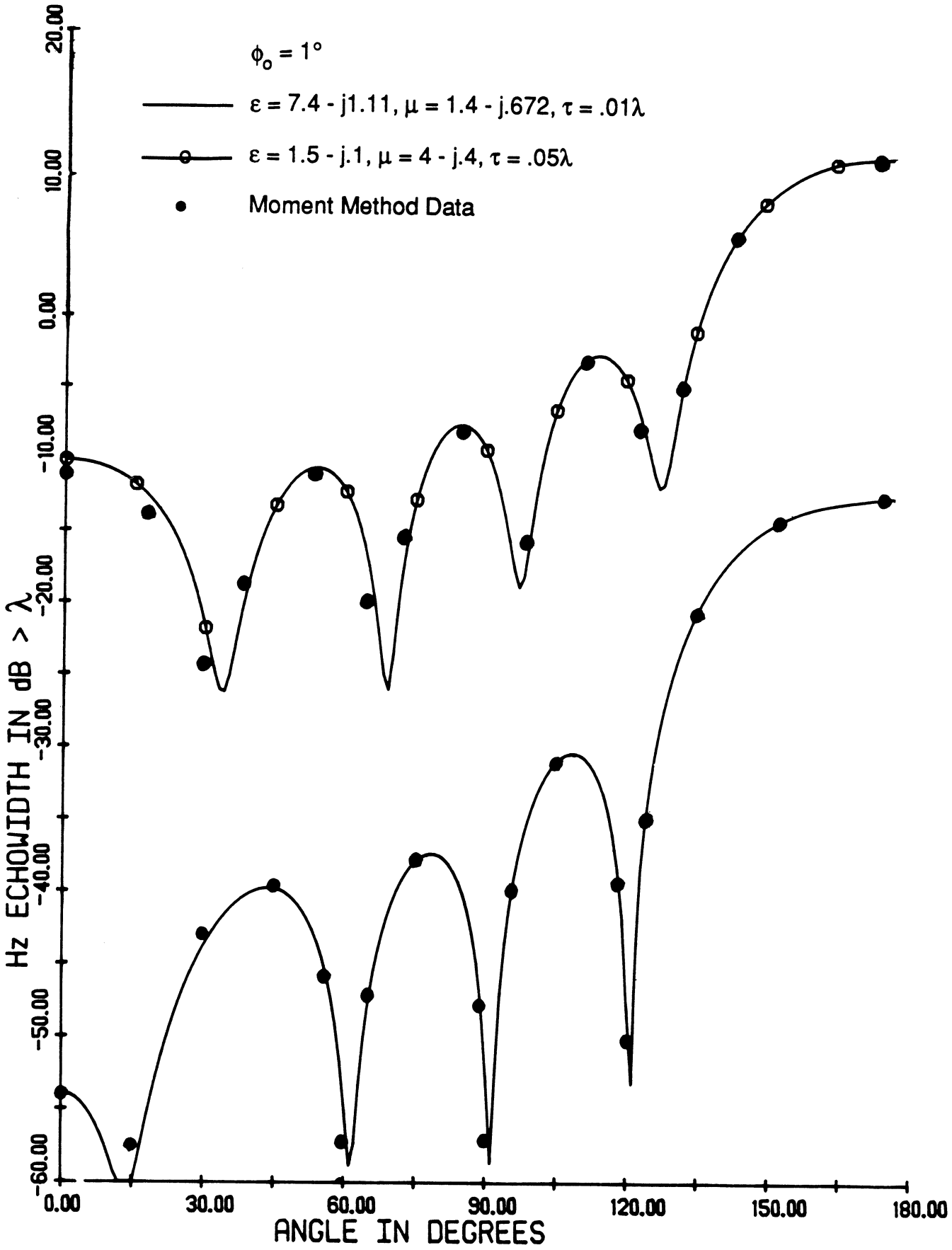

Fig. 11. H_z bistatic echowidth comparison of the high frequency solution versus moment method data for 2 wavelengths wide dielectric strips with ϕ_o, ε, μ and τ as indicated.

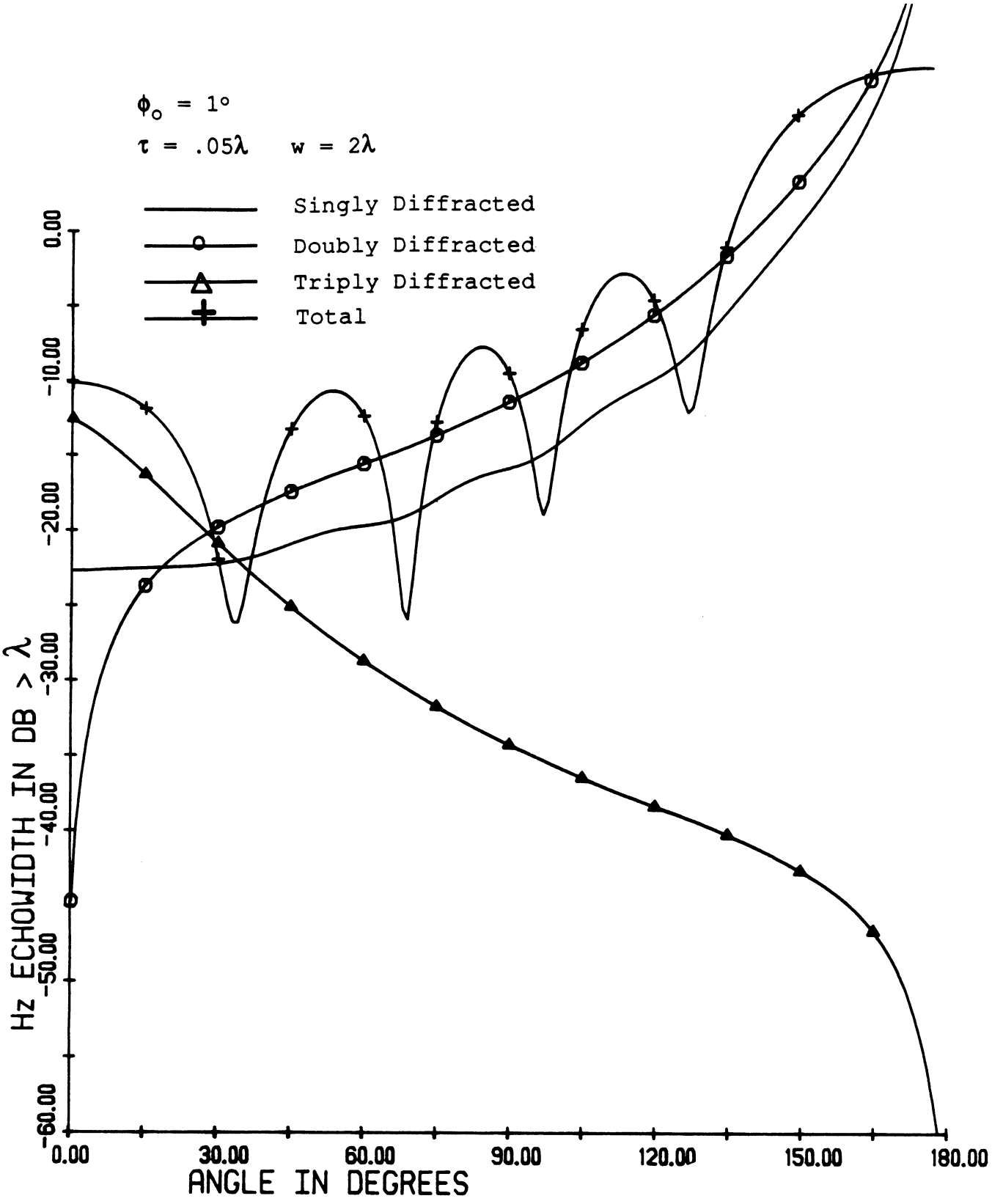

Fig. 12. Bistatic contribution of the multiply diffracted fields for the case of H_z-incidence on a 2 wavelengths wide and .05 wavelengths thick dielectric strip having $\varepsilon = 1.5 - j0.1$ and $\mu = 4 - j0.4$.

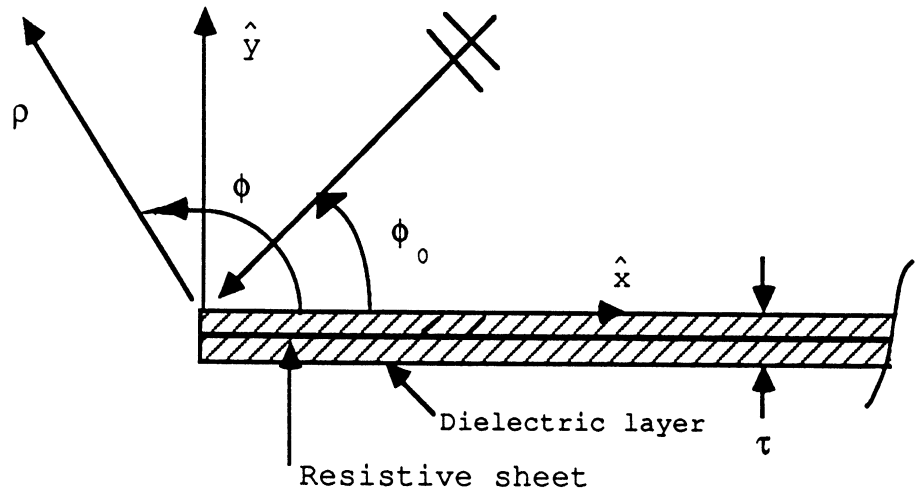

Fig. 13. Geometry of a resistive sheet imbedded in a dielectric layer